Virology 529 (2019) 91–100

Contents lists available at ScienceDirect

Virology

journal homepage: www.elsevier.com/locate/virology

Role of heparan sulfate in the Zika virus entry, replication, and cell death

Huixin Gao[a,b,1], Yuxia Lin[a,b,1], Junfang He[a,b], Shili Zhou[a,b], Mujiao Liang[a,b], Changbai Huang[a,b], Xiaobo Li[a,b], Chao Liu[a,b,*], Ping Zhang[a,b,*]

[a] Department of Immunology, Institute of Human Virology, Zhongshan School of Medicine, Sun Yat-sen University, Guangzhou 510080, China
[b] Key Laboratory of Tropical Diseases Control (Sun Yat-sen University), Ministry of Education, Guangzhou 510080, China

ARTICLE INFO

Keywords:
Heparan sulfate
Zika virus
Replication
Cell death

ABSTRACT

Zika virus (ZIKV) is an emerging arbovirus and its infection associates with neurologic diseases. Whether heparan sulfate (HS), an attachment factor for many viruses, plays a role in the ZIKV infection remains controversial. Our study generated several HS biosynthesis-deficient cell clones by disrupting *SLC35B2*, *B3GAT3*, or *B4GALT7* gene using the CRISPR/Cas9 system. The HS deficiency did not affect the viral attachment and internalization of ZIKV, but reduced the attachment of Dengue virus (DENV) 2. The early RNA and protein levels of ZIKV and DENV2 were impaired in the HS deficient cells, while the viral yields were not accordingly reduced. Our data further showed that HS promoted the cell death induced by virus infection, and inhibition of cell death significantly increased the viral replication of ZIKV and DENV2. Collectively, our study described an unexpected role of HS in the viral attachment, replication and cell death induced by ZIKV.

1. Introduction

Zika virus (ZIKV) is an emerging arbovirus of the *Flaviviridae* family, which includes a number of important arboviruses such as Dengue Virus (DENV), Japanese Encephalitis Virus (JEV), yellow fever virus (YFV), and West Nile Virus (WNV). Although the infection of ZIKV often leads to self-limiting diseases, it also causes severe neurologic disorders including microcephaly and Guillain–Barré syndrome (GBS). Nonetheless, no specific vaccine and drug is available for the treatment of these ZIKV diseases (Maslow, 2017; Pierson and Diamond, 2018; Saiz et al., 2018; Shan et al., 2018).

The infectious cycle of ZIKV starts with its binding to cellular receptors and attachment factors. Recent studies have revealed that ZIKV shares a bunch of cell surface receptors, including AXL, Tyro3, DC-SIGN, and TIM-1, with DENV for its entry (Hamel et al., 2015; Richard et al., 2017). However, none of these proteins has been validated to be unique, and physiologically relevant receptor of ZIKV (Miner and Diamond, 2017). Heparan sulfate (HS), a linear polysaccharide found in almost all animal tissues, has been identified as an attachment factor for several flaviviruses, including DENV (Chen et al., 1997), JEV (Chen et al., 2010), and YFV (Germi et al., 2002). HS is associated with proteins of cell surface and from extracellular matrix, and the long carbohydrate chains and negative charge of HS enable it to interact with positive-charged viral proteins. Not surprisingly, HS is employed as a nonspecific attachment factor by a number of viruses, including herpes simplex virus (Yura et al., 1992), HIV (Roderiquez et al., 1995), Semliki forest virus (Ferguson et al., 2015), foot-and-mouth disease virus (Fry et al., 1999), Sindibis virus (Byrnes and Griffin, 1998), Chikungunya virus (Silva et al., 2014; Tanaka et al., 2017), EV-A71 (Tan et al., 2013), vaccinia virus (Lin et al., 2000), adeno-associated virus type 2 virions (Summerford and Samulski, 1998), human respiratory syncytial virus (Feldman et al., 2000), Echoviruses (Goodfellow et al., 2001), Rabies virus (Sasaki et al., 2018), Coxsackievirus (Zhang et al., 2017), Akabane and Schmallenberg viruses (Murakami et al., 2017), and Rift Valley fever virus (Riblett et al., 2016).

Recently, Tan et al. (2017) reported that the ZIKV virus particles do not bind to heparin, a glycosaminoglycan that has similar protein-binding properties to HS, through a heparin binding assay. In contrast, Kim et al. (2017) showed that the recombinant ZIKV envelope protein interacts with various glycosaminoglycans including heparin through a surface plasmon resonance binding assay. To clarify these contradictory observations and to explore the role of HS in the interaction between ZIKV and host cells, our study utilized the CRISPR/Cas9 system to disrupt three key genes that encode proteins involved in the process of HS biosynthesis. Our data demonstrated that unlike DENV2, ZIKV did not rely on the HS for its entry. Unexpectedly, the early replication of

* Corresponding authors at: Department of Immunology, Institute of Human Virology, Zhongshan School of Medicine, Sun Yat-sen University, Guangzhou 510080, China.
E-mail addresses: liuchao9@mail.sysu.edu.cn (C. Liu), zhangp36@mail.sysu.edu.cn (P. Zhang).
[1] These authors contributed equally to this work.

https://doi.org/10.1016/j.virol.2019.01.019
Received 3 December 2018; Received in revised form 14 January 2019; Accepted 16 January 2019
Available online 18 January 2019

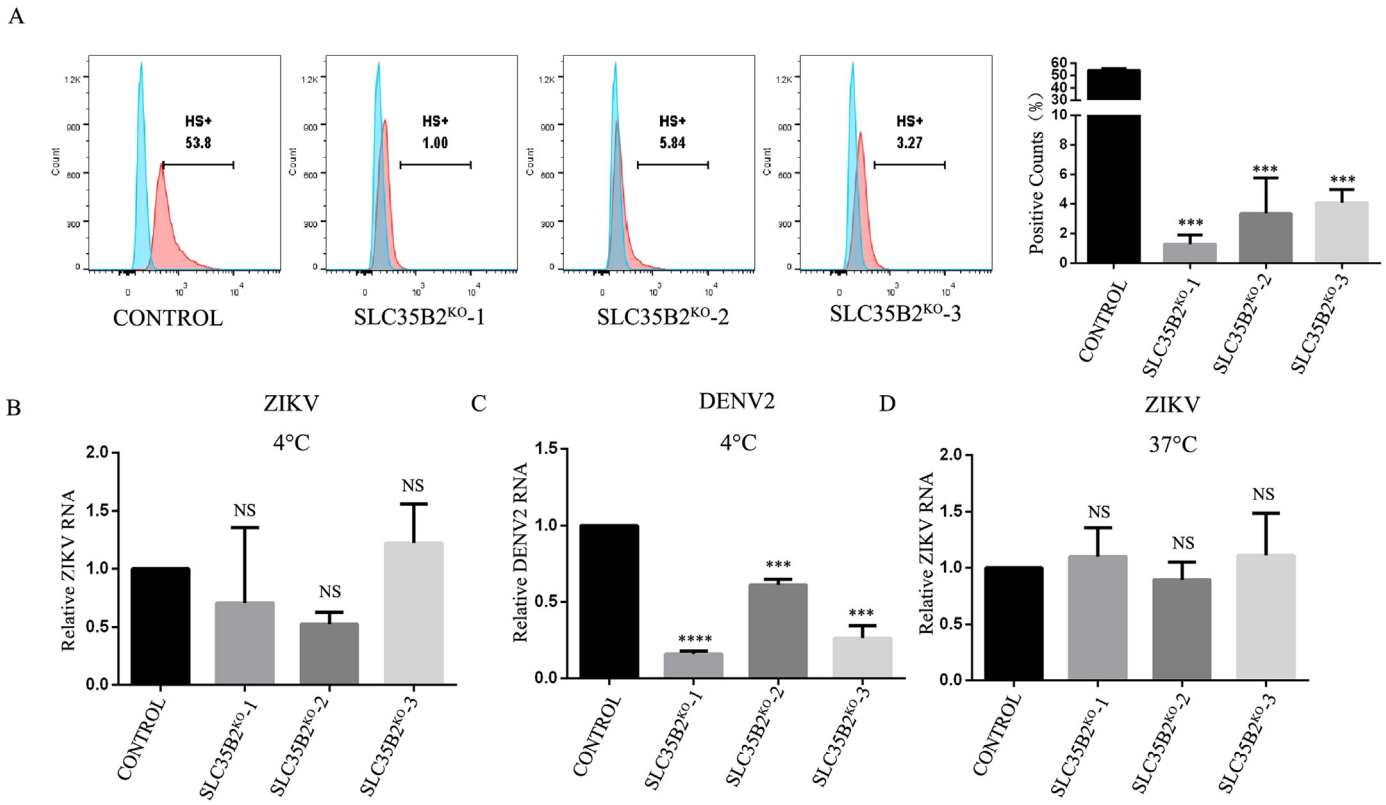

Fig. 1. The entry of ZIKV was not reduced in SLC35B2^{KO} cells. (A) Flow cytometry analysis of three SLC35B2^{KO} cell clones. The CRISPR/Cas9 mediated SLC35B2^{KO} cell clones were labeled with anti-HS antibody (blue) or with isotype control (red) and analyzed by flow cytometry. Representative data of three experiments were shown. (B, C) qRT-PCR analysis of viral RNA levels to indicate the amount of attached virions. The control cells and three SLC35B2^{KO} cells were infected with ZIKV at MOI 4 (B) or DENV2 at MOI 1 (C) at 4 °C for 1 h, followed by RNA extraction and qRT-PCR. (D) qRT-PCR analysis of viral RNA levels to indicate the amount of internalized virions. Control cells or three SLC35B2^{KO} cells were infected with ZIKV (MOI 4) at 37 °C for 30 min, followed by RNA extraction and qRT-PCR. Data were shown as mean ± SD of at least three independent experiments. NS, not significant, * **P < 0.001, * * *P < 0.0001, unpaired, two-tailed Student's *t*-test.

ZIKV was reduced in the HS deficient cells. We further revealed that HS had an impact on the ZIKV-induced apoptosis. These findings shed light on the roles of HS in the viral attachment, replication and cell death induced by ZIKV.

2. Materials and methods

2.1. Cell lines

Human lung carcinoma epithelial cells (A549, ATCC CCL-185), African green monkey kidney cells (Vero, ATCC CCL-81), baby hamster kidney cells (BHK21, ATCC CCL-10), and human embryonic kidney cells (293 T, ATCC CRL-3216) were maintained in Dulbecco Modified Eagle Medium (DMEM, Gibco) supplemented with 10% fetal bovine serum (FBS) (Gibco) at 37 °C with 5% CO_2. *Aedes albopictus* cells (C6/36, ATCC CRL-1660) were maintained in RPMI-1640 medium (Invitrogen) supplemented with 10% FBS at 28 °C with 5% CO_2. The media were added with 100 units/ml of streptomycin and penicillin (Invitrogen).

2.2. Viruses and viral titration

The ZIKV (H/PF/2013 strain) were provided by Dr. Michael Diamond at Washington University School of Medicine and propagated in Vero cells. Dengue 2 virus (DENV2) New Guinea C (NGC) strain were provided by Guangzhou Centers for Disease Control and propagated in C6/36 cells. Viral stocks were stored at −80 °C. Virus titers of ZIKV and DENV2 were determined by standard plaque assay on Vero or BHK21 cells. Visible plaques were counted at 3–4 days (ZIKV), 5–6 days (DENV2) post infection (p.i.).

2.3. Viral entry assay

The cells were incubated with ZIKV at an MOI of 4 or DENV2 at an MOI of 1 at 4 °C for 1 h, during which ZIKV or DENV2 attach to cell surface but not enter the cell. In the internalization assay, the cells were incubated with ZIKV at an MOI of 4 at 37 °C for 30 min. The supernatant was then removed and the cells were extensively washed three times with cold PBS. Total RNA was extracted using Trizol (Invitrogen) and then ZIKV or DENV2 RNA levels were measured by qRT-PCR.

2.4. Quantitative reverse transcription-PCR (qRT–PCR)

Total RNA was reverse transcribed using HI Script Q RT SuperMix (Vazyme). qRT–PCR was performed using the cDNA templates and the SYBR Select Master Mix for CFX (Applied Bio systems) in Bio-Rad CFX96 machine. The following primers were used in this study: ZIKV-5F: GTCAGAGCAGCAAAGACAA; ZIKV-3R: CAGCCTCCTTTCCCTTAACA; DENV2–5F: TCCTAACAATCCCACCAACAGCA; DENV2–3R: AGTTCTGCGTCTCCTGTTCAAGA. The PCR data were analyzed using SDS software (Applied Biosystems). Actin level was measured as an internal control.

2.5. Generation of SLC35B2, B3GAT3, and B4GALT7 gene-disrupted cell clones

SLC35B2, *B3GAT3*, and *B4GALT7* gene-disrupted cell clones were generated by CRISPR/Cas9 system (Ran et al., 2013). sgRNAs were designed and cloned into the lentiCRIPSR v2 (Addgene #52961). The sgRNA sequences were as follows: SLC35B2, 5′-AGAGTGATGACCCGCAGCTA-3′ and 5′-TAGCTGCGGGTCATCACTCT-3′; B3GAT3, 5′-TTCCC

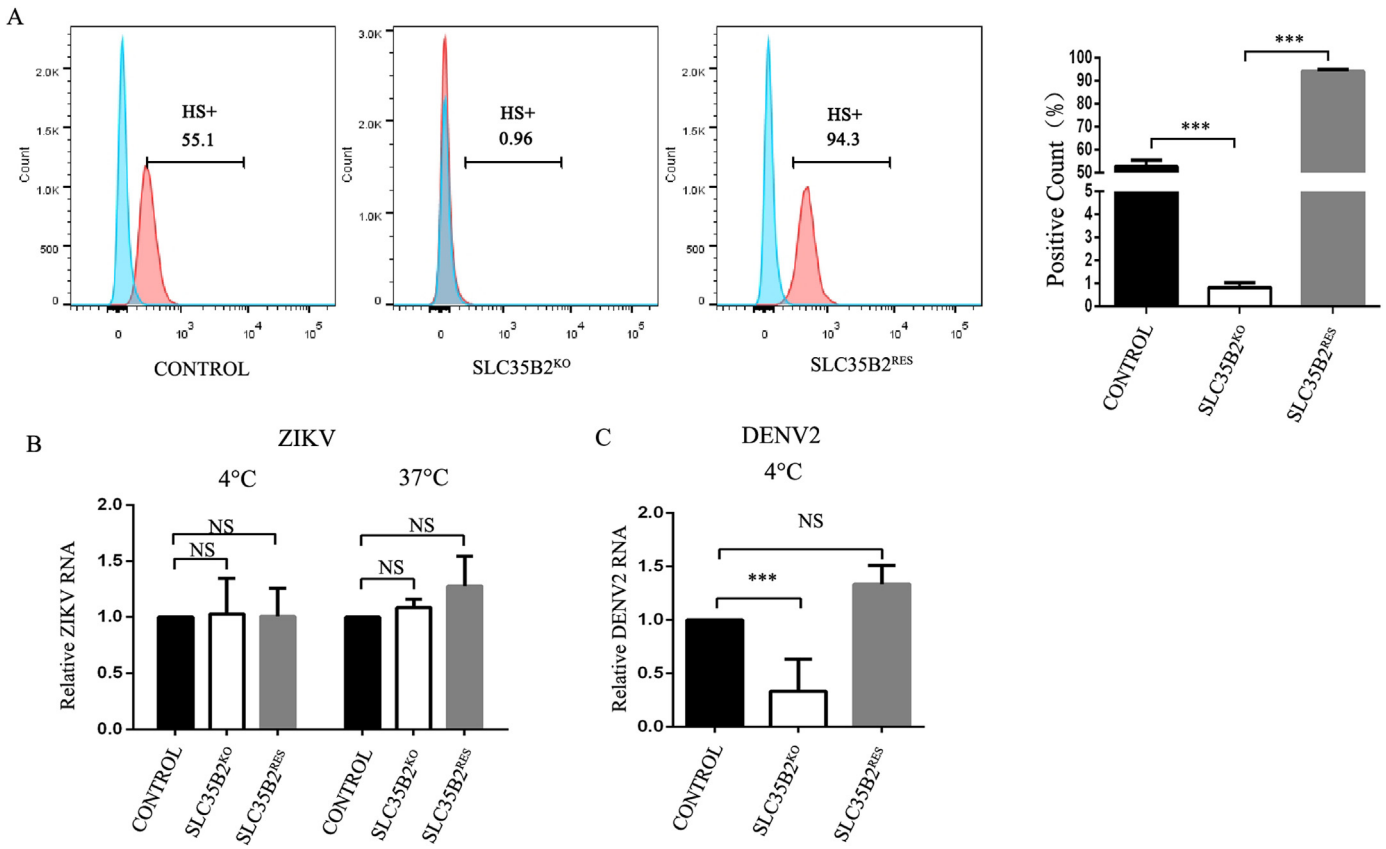

Fig. 2. Effect of the SLC35B2 add-back in SLC35B2^{KO} cells in viral entry. (A) Flow cytometry analysis. The control, SLC35B2^{KO}, and SLC35B2^{RES} cell clones were labeled with anti-HS antibody (blue) or with isotype control (red) and analyzed by flow cytometry. Representative data of three experiments were shown. (B, C) qRT-PCR analysis of viral RNA levels to indicate the amount of attached virions. The control, SLC35B2^{KO}, and SLC35B2^{RES} cells were infected with ZIKV at MOI 4 (B) or DENV2 at MOI 1 (C) at 4 °C for 1 h or 37 °C for 30 min, followed by RNA extraction and qRT-PCR. Data were shown as mean ± SD of at least three independent experiments. NS, not significant, * **P < 0.001, unpaired, two-tailed Student's *t*-test.

TTACCCGAGTGCAGT-3′ and 5′-ACTGCACTCGGGTAAGGGAA-3′; B4GALT7, 5′-CAGCAGGATGCCGCCGACAT-3′ and 5′-ATGTCGGCGGC ATCCTGCTG-3′. The lentivirus was packaged in 293 T cells. 400 ng lentiCRISPR v2 containing sgRNA, 400 ng pSPAX2 (Addgene #12260), and 200 ng pMD2. G (Addgene #12259) were introduced into 293 T cells (12-well plate) using FuGENE® HD Reagent (Promega). After 2 days, culture supernatants were passed through a 0.45 μm filter, and used for gene transduction. A549 cells were transduced with lentivirus carrying sgRNA and selected by puromycin (1 μg/ml), and single clones were isolated. The cell clones were confirmed by genome DNA extraction and sequencing (Ran et al., 2013). The sequencing primers were as follows: SLC35B2, 5′-GGCTACCTCCTGGTGCAGTAC-3′ and 5′-ACAGGGATCACCTTAGAGGCC T-3′; B3GAT3, 5′-TGGTTAGCAGTGT TGCCGTTGG-3′ and 5′-CAGGGCCTTATTCCTTCATCCTCTC-3′; B4GALT7, 5′-TGCTGTACCTCCCGTGCTTTGA-3′ and 5′-CAGGGTCCTG GTGACACTGTCTGA-3′.

2.6. Generation of SLC35B2^{RES} cells

The SLC35B2 gene fragment was amplified by PCR (primer sequence: 5′-ATAAGAATGCGGCCGCATGGTGGGCAGTGGTGGTGCTG-3′ and 5′-GCGGGATCCTCAAACCTTCTGCACAGGAGAC-3′) and cloned into the lentivirus vector CSII-EF-MCS-IRES2-Venus (Riken). The lentivirus was packaged in 293 T cells. Cells were transfected with CSII-EF-MCS-IRES2-Venus–SLC35B2, pSPAX2, and pMD2. G using FuGENE® HD Reagent (Promega). After 2 days, culture supernatants were passed through a 0.45 μm filter, and used for gene transduction. The SLC35B2^{KO} cells were transduced with lentivirus carrying SLC35B2 gene, and Venus positive cells were sorted by flow cytometry (CytoFLEX). The purity of SLC35B2^{RES} was estimated to be more than 80%.

2.7. Flow cytometry analysis

The control cells, SLC35B2, B3GAT3, and B4GALT7 gene-disrupted cell clones were detached with PBS containing EDTA and incubated with anti-heparan sulfate monoclonal antibody (10E4, USBio), followed by incubation with Alexa Fluor 488-conjugated anti-mouse IgM antibody (Invitrogen). Labeled cells were analyzed by flow cytometry (LSRFORTESA, BD).

2.8. MTT assay

MTT (3-(4,5)-dimethylthiahiazo (-z-y1)-3,5-di- phenytetrazoliumromide, Genview) was added to cell culture (5 mg/ml dissolved in PBS) and incubated for 4 h at 37 °C. MTT was reduced by live cells into a colored formazan product. After centrifugation at 1500 rpm for 5 min, the supernatant was discarded and DMSO was added to the plate, which was gently shaken for 10 min to dissolve the formazan product. OD value was measured at 490 nm using a BioTek Instrument (BioTek).

2.9. Western blot

Whole cell extracts were prepared in the presence of 1 mM PMSF, 1% (v/v) protease inhibitor cocktail (Sigma) and DDT. Proteins were fractionated by electrophoresis on sodium dodecyl sulfate-10% polyacrylamide gels, and transferred to nitrocellulose membranes. The

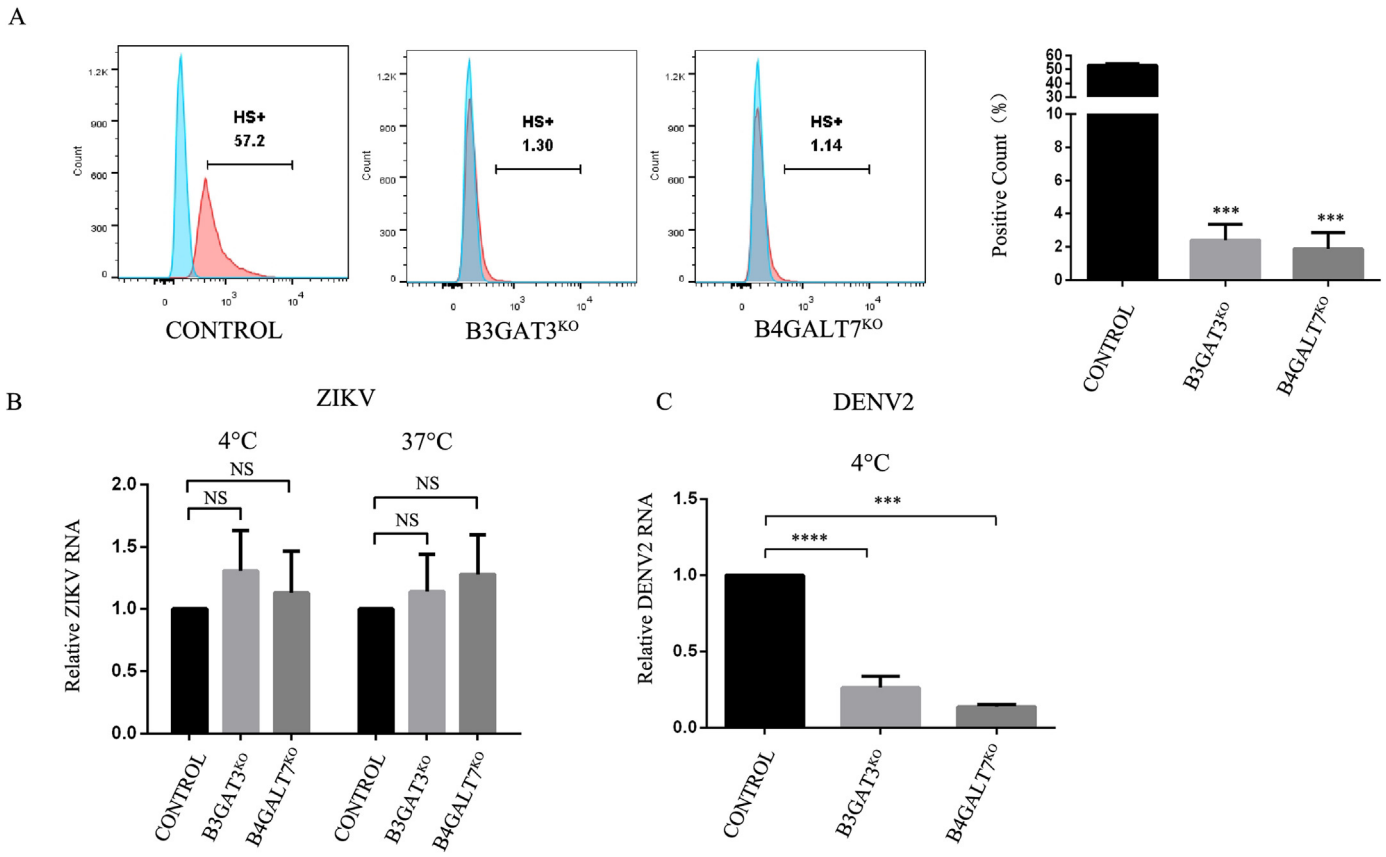

Fig. 3. The entry of ZIKV was not reduced in another two HS-deficient cells. (A) Flow cytometry analysis. The control, B3GAT3^{KO}, and B4GALT7^{KO} cell clones were labeled with anti-HS antibody (blue) or with isotype control (red) and analyzed by flow cytometry. Representative data of three experiments were shown. (B, C) qRT-PCR analysis. The control, B3GAT3^{KO}, and B4GALT7^{KO} cells were infected with ZIKV at MOI 4 (B) or DENV2 at MOI 1 (C) at 4 °C for 1 h or 37 °C for 30 min, followed by RNA extraction and qRT-PCR. Data were shown as mean ± SD of at least three independent experiments. NS, not significant, * **P < 0.001, * * **P < 0.0001, unpaired, two-tailed Student's *t*-test.

membranes were blocked, and probed with primary antibodies at 4 °C overnight. Detection was performed with IRDye 800 CW–conjugated anti-rabbit IgG or IRDye 680 LT–conjugated anti-mouse IgG secondary antibody according to the manufacturer's protocols (LI-COR). Immunoreactive bands were visualized using an Odyssey infrared imaging system (LI-COR). Primary antibodies GAPDH (Proteintech), ZIKV E (BioFront), DENV2 NS3 (Sigma), PKR (Santa Cruz Biotechnology), PARP (Cell Signaling Technology), and secondary antibodies IRDye 800 CW–conjugated anti-rabbit IgG and IRDye 680 LT–conjugated anti-mouse IgG (LI-COR) were used.

2.10. Treatment of inhibitors

A pan-caspase inhibitor of apoptosis, z-VAD(OMe)-FMK (MCE), and a specific inhibitor of necrosis, Necrostatin-1 (MCE), were dissolved in DMSO at a stock concentration of 100 mM. The working solution was freshly prepared in 50 μM (z-VAD(OMe)-FMK) or 100 μM (Necrostatin-1) concentrations. Growth media and 0.1% DMSO were used as parental and vehicle controls respectively. A549 cells were pretreated with z-VAD(OMe)-FMK, Necrostatin-1 or their combination for 1 h , and then infected with ZIKV at an MOI of 4, or DENV2 at an MOI of 1. Cell viability was measured by the MTT assay. At 24 h p.i., cell morphology was monitored using phase contrast light microscopy (Leica DMI8).

2.11. Treatment of IFN-β or poly(I:C)

IFN-β (Proteintech) was dissolved in PBS at a stock concentration of 500 units/μl. A549 cells were left untreated or treated with 1000 units/ml IFN-β in DMEM supplemented with 10% FBS for 24 h. The cell viability was measured by the MTT assay, or the whole cell extracts were prepared for western blot.

A549 cells were transfected with mock or 1 μg/ml poly(I:C) (Sigma) using Lipofectamine 2000 Reagent (Invitrogen) following the manufacturer's instruction. At 12 h post transfection, the whole cell extracts were collected for western blot.

2.12. Statistical analysis

All experiments were independently repeated at least three times. Comparisons between two groups were performed using Student's *t*-test. Graphs were generated using Graph Pad Prism 6.0 software. P values of 0.05 or lower were considered to be statistically significant.

3. Results

3.1. Heparan sulfate was indispensable for the entry of Zika virus

To examine whether HS plays a role in the ZIKV infection, we generated *SLC35B2* gene-disrupted cell clones through the CRISPR/Cas9 system. The SLC35B2 protein is a transporter of 3-prime-phosphoadenosine 5-prime-phosphosulfate (PAPS) which is a sulfate donor for sulfation of HS (Kreuger and Kjellen, 2012). Disruption of *SLC35B2* gene was confirmed by genome DNA sequencing. Three SLC35B2 gene-disrupted cell clones were selected and designated as SLC35B2^{KO-1}, SLC35B2^{KO-2}, and SLC35B2^{KO-3}. We first measured the surface HS expression in these KO cells by flow cytometry. The percentages of SLC35B2^{KO-1}, SLC35B2^{KO-2}, or SLC35B2^{KO-3} cells that stained with HS were greatly reduced (around 1.00%, 5.84%, and 3.27%

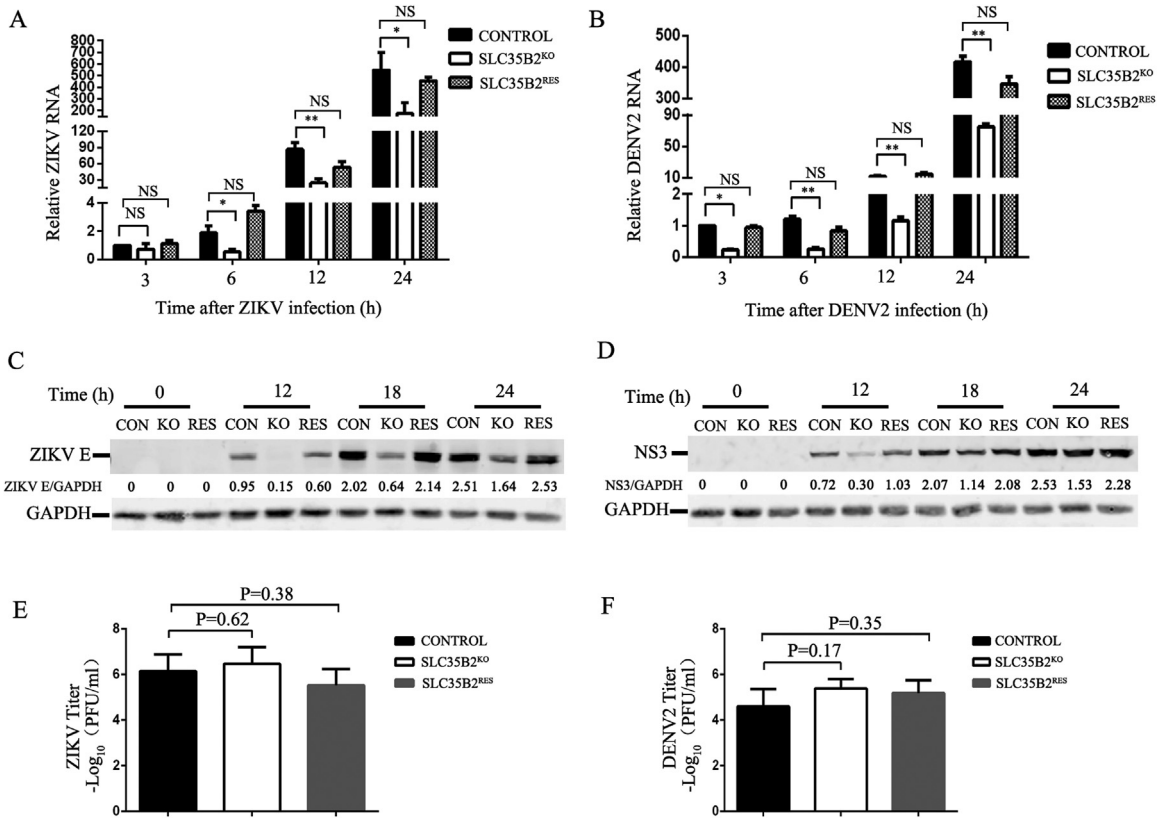

Fig. 4. Role of HS in ZIKV and DENV2 replication. The control, SLC35B2^{KO}, and SLC35B2^{RES} cell clones were infected with ZIKV (MOI 4) or DENV2 (MOI 1). (A, B) qRT-PCR analysis of kinetic viral RNA levels. Total RNA were extracted at 3, 6, 12 or 24 h p.i., and applied for qRT-PCR. (C, D) Western blot analysis of viral protein levels. Cells were harvested at 0, 12, 18 or 24 h p.i. for whole cell extract preparation and western blot to detect ZIKV E protein or DENV2 NS3 protein. GAPDH was probed as an internal control. (E, F) Virus titers. The supernatants of infected cells were collected at 24 p.i. for virus titration by plaque assay. Data were shown as mean ± SD of at least three independent experiments. P values were calculated by unpaired, *P < 0.05, **P < 0.01, two-tailed Student's *t*-test.

respectively), while 53.8% of the control cells were positively stained with HS (Fig. 1A). To determine whether HS is involved for viral attachment, we exposed the control cells, three SLC35B2^{KO} cells to ZIKV or DENV2 for 1 h at 4 °C, and then employed a qRT-PCR assay to measure the RNA levels of attached virions. As shown in Fig. 1B, the viral RNA levels of ZIKV in all tested cells were comparable (P > 0.05). In contrast, the viral RNA levels of DENV2 attached to the SLC35B2^{KO} cell clones were significantly lower than in control cells (all P < 0.001, Fig. 1C), consistent with previous studies (Chen et al., 1997; Germi et al., 2002). Then, we examined the HS involvement in ZIKV internalization by inoculating the ZIKV on control cells and SLC35B2^{KO} cells for 30 min at 37 °C to allow virions to attach and internalize. The qRT-PCR data showed that the viral RNA levels in all three SLC35B2^{KO} cell clones were similar to the control cells, indicating the amounts of internalized virions were not altered (Fig. 1D).

To further confirm the role of HS in the viral entry, we transduced the SLC35B2^{KO-1} cells with the *SLC35B2* gene and generated SLC35B2 add-back cells (SLC35B2^{RES}). The flow cytometry data showed that the expression of HS was fully recovered in SLC35B2^{RES} cells (Fig. 2A). In the SLC35B2^{RES} cells, the viral RNA levels of ZIKV that exposed to cells at 4 °C or 37 °C were both comparable to the control cells or SLC35B2^{KO} cells (Fig. 2B), while the RNA levels of DENV2 that attached to SLC35B2^{RES} cells was largely restored (Fig. 2C).

In addition, we utilized CRISPR/Cas9 system to generate another two cell clones that did not express B3GAT3 or B4GALT7 proteins, which function as glucuronosyltransferase I and galactosyltransferase I respectively in the HS biosynthesis pathway (Kreuger and Kjellen, 2012). The flow cytometry data showed that the percentages of HS-staining cells were significantly reduced in these cell clones (around 1.30% and 1.14%), which were designated as B3GAT3^{KO} and B4GALT7^{KO} respectively (Fig. 3A). We then compared the viral attachment and internalization levels in the control cells, B3GAT3^{KO}, and B4GALT7^{KO} cells. We did not observe a significant alteration of ZIKV RNA levels between the control and knockout cells either incubated at 4 °C or 37 °C (all P > 0.05, Fig. 3B). In contrast, the viral RNA levels of DENV2 that attached to the B3GAT3^{KO} and B4GALT7^{KO} cells were largely reduced (all P < 0.00.1, Fig. 3C). These data indicated that unlike DENV2, HS was not required for ZIKV for its attachment and endocytosis.

3.2. The early replication levels of ZIKV were downregulated in the HS deficient cells

To explore whether HS regulates the ZIKV replication, we compared the viral RNA levels, protein expression, and viral yields in the HS sufficient cells (control and SLC35B2^{RES}) and the HS deficient cells (SLC35B2^{KO}) through qRT-PCR, western blot, and plaque assay. Cells were infected with ZIKV (MOI 4) or DENV2 (MOI 1), and harvested at 3, 6, 12, and 24 h post infection (p.i.) for qRT-PCR. The ZIKV RNA levels at 3 h p.i. were comparable among these three cells, while the viral RNA levels in the SLC35B2^{KO} cells were significantly reduced at 6, 12, and 24 h p.i. compared to the control and SLC35B2^{RES} cells (Fig. 4A). The DENV2 RNA levels in SLC35B2^{KO} cells were significantly reduced as early as at 3 h p.i., and throughout all the later time points (Fig. 4B). The western blot analysis showed that the ZIKV E protein levels in the SLC35B2^{KO} cells were dramatically lower than the control cells and SLC35B2^{RES} at 12, 18, and 24 h p.i. (Fig. 4C). Likewise, the DENV2 NS3 levels at 12 and 18 h p.i. were impaired in the SLC35B2^{KO} cells, but its level was increased to a similar level to the control cells at 24 h p.i. (Fig. 4D). Next, we harvested the supernatants at 24 h p.i., and titered

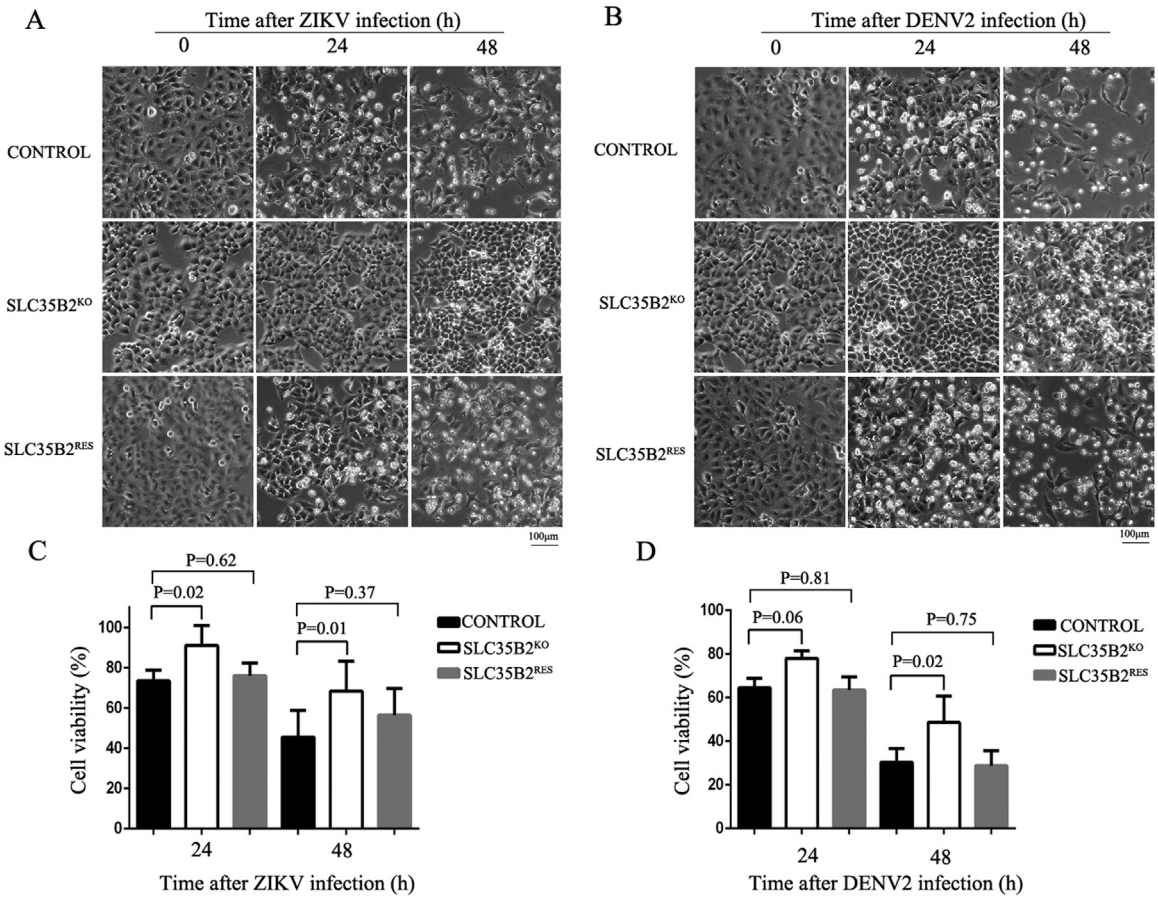

Fig. 5. Role of HS in the cell death induced by ZIKV and DENV2 infection. The control, SLC35B2^{KO}, and SLC35B2^{RES} cells were infected with ZIKV (MOI 4) or DENV2 (MOI 1). (A, B) Cell images were taken at 0, 24, and 48 h p.i. (C, D) Cell viabilities of the mock- and virus-infected cells at 24 and 48 h p.i. measured by MTT assay. Data were shown as mean ± SD of at least three independent experiments. P values were calculated by unpaired, two-tailed Student's *t*-test.

them by plaque assay. Surprisingly, the viral yields of both ZIKV and DENV2 were comparable in the control, SLC35B2^{KO} and SLC35B2^{RES} cells ($P > 0.05$, Fig. 4E and F). Altogether, our data indicated that HS plays a role in the early viral replication of ZIKV.

3.3. The HS deficiency decreased the cell death induced by ZIKV and DENV2 infection

Surprisingly, no notable cytopathic effect were observed in the ZIKV-infected SLC35B2^{KO} cells, unlike the control cells. To probe whether HS plays a role in the cell death induced by virus infection, we monitored the morphology and viability of cells infected with mock or viruses. The control cells, SLC35B2^{KO}, and SLC35B2^{RES} cells were infected by ZIKV (MOI 4) or DENV2 (MOI 1), and the cell images were taken at 24 and 48 h p.i.. Fig. 5A clearly showed that the control and SLC35B2^{RES} cells showed characteristics of cell death including cell membrane blebbing, cell shrinkage and detachment upon ZIKV infection, and the extent of cell death increased with time lapsed. In contrast, the morphology of most SLC35B2^{KO} cells remained intact upon ZIKV infection, barely showing cytopathic effect. Similarly, in response to DENV2 infection, severe cytopathic effect was observed in the HS sufficient cells, but not in the HS deficient cells at 24 and 48 h p.i. (Fig. 5B).

Next, we performed the MTT assay to quantitate the cell viability. At 24 h p.i., the ZIKV and DENV2 infection led to 27.5% and 35.5% cell death in the control and SLC35B2^{RES} cells, but only 8.9% and 22.0% cells underwent cell death in the SLC35B2^{KO} cells; at 48 h p.i., the differences of cell viability between control cells and SLC35B2^{KO} cells were even more significantly ($P < 0.05$, Fig. 5C and D). These data suggested that HS was involved in the cell death induced by ZIKV and DENV2 infection.

3.4. The viral replication levels of ZIKV and DENV2 were upregulated by inhibition of cell death

The lacking of HS largely downregulated the early RNA and protein levels (6, 12, and 18 h p.i.), but had a limited impact on the viral replication levels at 24 h p.i.. Together with the observation that HS promotes the cell death, we hypothesized that less cell death seen in the HS-deficient cells is responsible for the increased ZIKV replication at 24 h p.i.. To test this hypothesis, we utilized two inhibitors, namely pan-caspase inhibitor z-VAD(OMe)-FMK to inhibit the apoptosis, and RIP1 inhibitor Necrostatin-1 to inhibit the necrosis, as ZIKV and DENV2 could induce apoptosis and necrosis (Oh et al., 2017; Vicenzi et al., 2018). The control, SLC35B2^{KO}, and SLC35B2^{RES} cells were infected with ZIKV or DENV2 in the presence of vehicle, z-VAD(OMe)-FMK, Necrostatin-1, or their combination. At 24 h p.i., the cell images were taken and the cell viabilities were measured by the MTT assay. In response to ZIKV or DENV2 infection, the cell death was observed in the control cells (left panels, Fig. 6A), which was significantly alleviated in the presence of z-VAD(OMe)-FMK, Necrostatin-1 or their combination (Fig. 6A). As expected, the morphology of infected SLC35B2^{KO} cells did not show significant alteration in the presence of individual or double inhibitors. Consistently, the MTT data showed that the treatment of z-VAD(OMe)-FMK, Necrostatin-1 or both inhibitors increased the cell viability of control or SLC35B2^{RES} cells upon ZIKV (Fig. 6B) or DENV2 (Fig. 6C) infection. Interestingly, the treatment of the Necrostatin-1, but not z-VAD(OMe)-FMK led to enhancement of cell viability of the

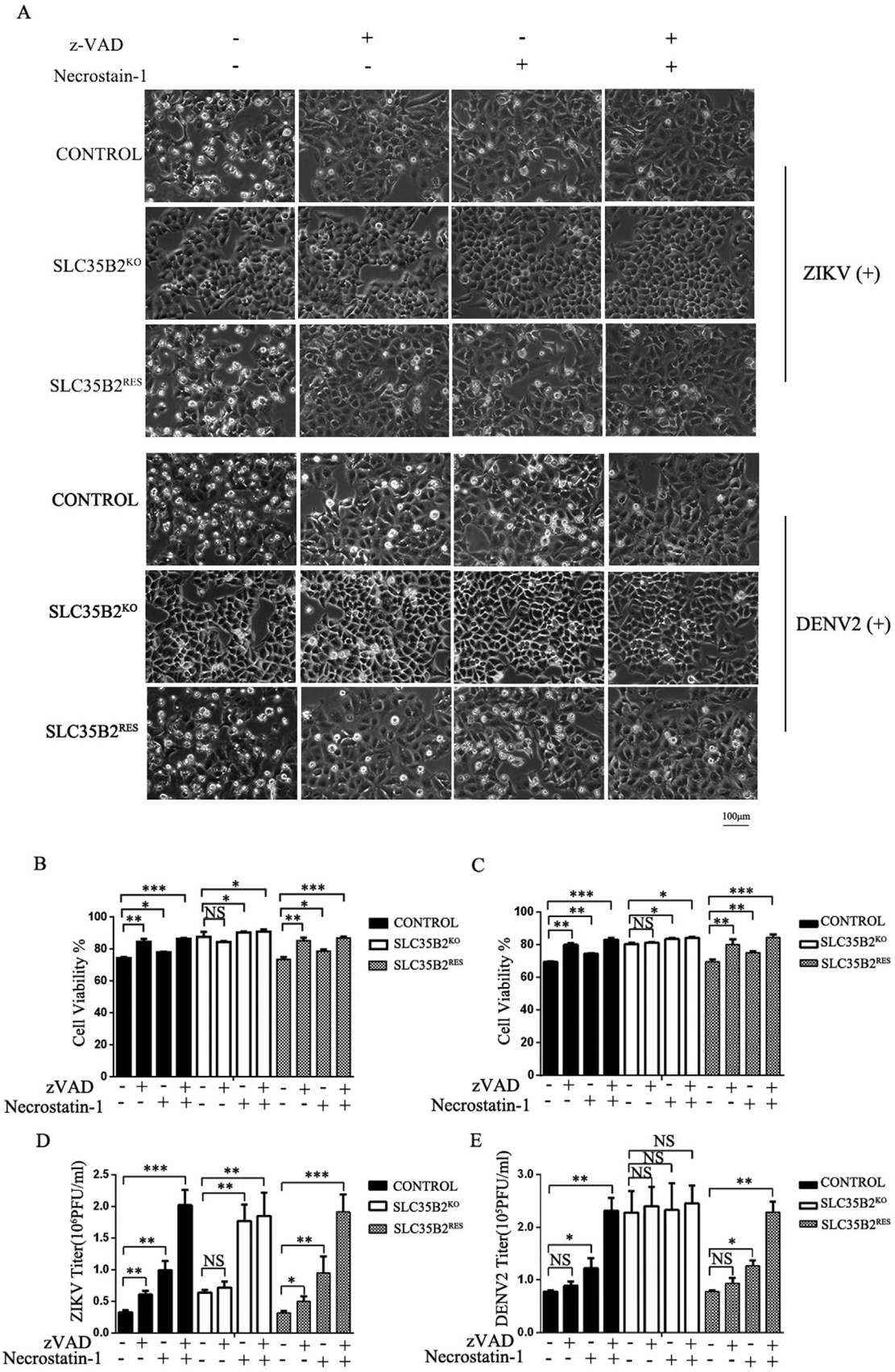

Fig. 6. Inhibition of cell death restored the viral production. The control, SLC35B2^{KO}, and SLC35B2^{RES} cell clones were pretreated with z-VAD(OMe)-FMK, Necrostatin-1 or their combination for 1 h, followed by infection of ZIKV (MOI 4) or DENV2 (MOI 1). At 24 h p.i., the cells or supernatant were harvested for following assays. (A) Cell images. (B, C) MTT assay to measure the cell viabilities. (D, E) Plaque assay to measure virus titers. Data were shown as mean ± SD of at least three independent experiments. NS, not significant, *P < 0.05, **P < 0.01, ***P < 0.001, unpaired, two-tailed Student's *t*-test.

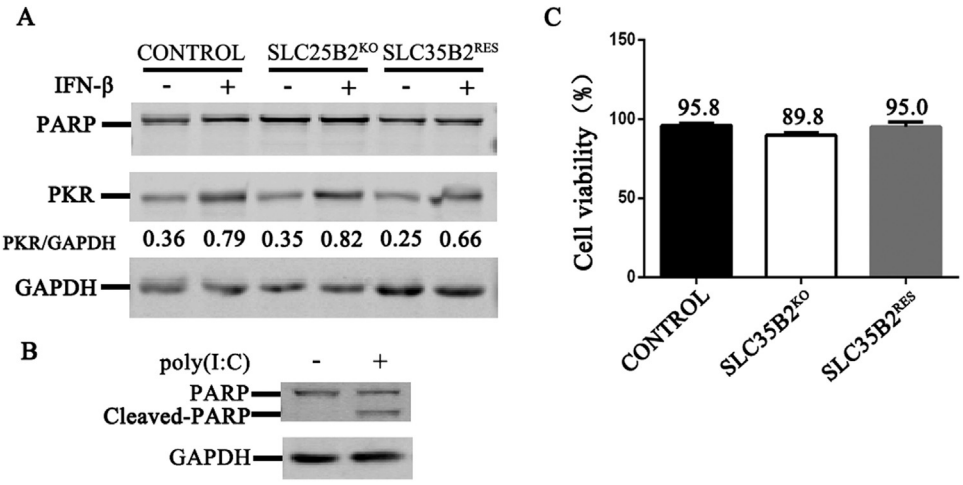

Fig. 7. Role of HS in the apoptosis and cell viability treated by IFN-β. (A, B), Western blot. The control, SLC35B2^{KO}, and SLC35B2^{RES} cells were treated with 1000 units/ml IFN-β for 24 h. Whole cell extracts were prepared at 24 h p.i. for western blot to detect the levels of PARP and PKR (A). Or A549 cell were transfected with poly(I:C) for 12 h and then subjected for western blot to detect the level of PARP (B). GAPDH was probed as an internal control. (C), Cell viabilities measured by MTT assay. Cells were treated with 1000 unit/ml IFN-β for 24 h and harvested for MTT assay. Data were shown as mean ± SD of at least three independent experiments. P values were calculated by unpaired, two-tailed Student's *t*-test.

SLC35B2^{KO} cells, implying that HS was not involved in the cell necrosis (Fig. 6B and C).

Next, we performed plaque assay to test whether the virus titers were restored by the treatment of cell death inhibitors. The virus yields of ZIKV and DENV2 in the control and SLC35B2^{RES} cells were significantly increased by treatment of z-VAD(OMe)-FMK, Necrostatin-1, or their combination, with an exception of DENV2 titer in cells treated with z-VAD(OMe)-FMK (Fig. 6D and E). Particularly, the combination of two inhibitors led to 6.1- and 3.0-fold induction of ZIKV or DENV2 yields, indicating that cell death is an effective antiviral strategy of host cell. In the SLC35B2^{KO} cells, an elevation of ZIKV yield was observed in the presence of Necrostatin-1 (white bars, Fig. 6D), in keeping with the enhancement of cell viability of the SLC35B2^{KO} cell treated with Necrostatin-1. These data confirmed that both of apoptosis and necrosis induced by ZIKV and DENV2 infection play a protective role, also suggesting that HS is mainly involved in the apoptosis pathway.

3.5. The proapoptotic effect of HS did not rely on the IFN-β

The HS and heparin has been indicated to bind to a number of pro-apoptotic cytokines and growth factors (Lortat-Jacob, 2006; Salas et al., 2000). As our Qrt-PCR and microarray data showed that the IFN-β was highly induced in the ZIKV-infected cells (data not shown), and the IFN-β induces the apoptosis in melanomas, ovarian carcinoma, and multiple myeloma (Chawla-Sarkar et al., 2003), we further tested whether the HS promotes the ZIKV-induced apoptosis through binding to the IFN-β. The control, SLC35B2^{KO} and SLC35B2^{RES} cells were treated with IFN-β for 24 h, and collected for western blot and MTT assays. The western blot data showed that the PARP protein, an indicator of apoptosis, was not cleaved in all of tested samples, suggesting that no apoptosis occurred at 24 h post IFN-β treatment (Fig. 7A). As a control, the poly(I:C) treatment readily led to the PARP cleavage in A549 cells (Fig. 7B). The levels of PKR, a classic IFN stimulated gene, were similarly upregulated by IFN-β in these cells, demonstrating that the IFN treatment was effective, and the IFN signaling pathway was not inhibited by the HS deficiency (Fig. 7A). Consistent with the finding that the IFNs had an inhibitory effect on the cell proliferation (Balkwill and Taylor-Papadimitriou, 1978), the cell viabilities of IFN-treated cells were generally lower than the mock-treated cells, but the HS KO did not lead to a higher cell viability ($P > 0.05$, Fig. 7C), suggesting that the proapoptotic effect of HS was independent of the type I IFNs.

4. Discussion

Heparan sulfate has been identified to be an attachment factor for several flaviviruses, including DENV, YFV, and JEV (Chen et al., 2010, 1997; Germi et al., 2002). However, roles of HS in the ZIKV infection, especially its replication beyond the attachment remained largely unknown (Kim et al., 2017; Tan et al., 2017). Current study addressed this question through generating the HS biosynthesis deficient cells by the CRISPR/Cas9 gene editing system. Our data showed that although HS is not essential in the viral entry of ZIKV, it plays a role in the viral replication and cell death.

Our data provided several pieces of evidence that HS is dispensable in the ZIKV entry. First, the amounts of ZIKV particles attached on the cell surface and internalized were not reduced in the three SLC35B2^{KO}, B3GAT3^{KO}, and B4GALT7^{KO} cells. In contrast, the amounts of DENV2 particles attached on these HS deficient cells were dramatically reduced, confirming the notion that HS is an attachment factor for DENV entry (Chen et al., 1997; Germi et al., 2002). Secondly, the add-back of SLC35B2 gene in the SLC35B2^{KO} cells did not change the levels of ZIKV attachment and endocytosis. Thirdly, the viral RNA levels at 3 h p.i. were comparable in the control cells and the SLC35B2^{KO} cells, indicating that the amount of ZIKV RNA released into the cytoplasm was not reduced by HS deficiency. Although ZIKV shares many cell surface molecules such as DC-SIGN, and AXL with DENV (Hamel et al., 2015), their requirements on HS are differential. ZIKV might utilize alternative attachment factors for its attachment. As the interaction of virus with its cellular surface factors is a key determinant for the virus transmission and tissue tropism, we postulate that the attachment factors for ZIKV in neural system might be more abundant than in other tissues.

Our finding supported the conclusion that HS is not required for ZIKV attachment (Tan et al., 2017). Tan et al. (2017) showed that the majority of ZIKV viral particles were not retained by heparin sepharose, and the inhibition of cell sulfation by sodium chlorate or the removal of HS by heparinase I/III did not affect viral infectivity, suggesting the virus does not bind HS. In another report, Kim et al. (2017) carried out in vitro biochemistry assay to show the kinetic interaction between the recombinant ZIKV envelope protein and purified heparin. The different systems utilized in these studies might attribute to these contradictory observations. The interaction between the whole viral particles and cells utilized by Tan et al. and us, is presumably more complex than the in vitro protein-protein interaction employed by Kim et al., since many other cellular and viral molecules might be involved in. Nonetheless, the cell-based system provides a more physiological context, and other relevant factors need to be further explored. In the study to test the requirement of HS for DENV entry, Chen et al. (1997) consistently observed that DENV E protein binds to a highly sulfated type of HS from in vitro binding assay, and that HS and heparin inhibit the DENV infectivity from the cell assay, which was also demonstrated by our data using HS-deficient cells.

An unexpected observation is that the viral RNA and protein levels of ZIKV and DENV2 at early stage (6, 12, and 18 h p.i.) were significantly decreased in the HS deficient cells. Given the ZIKV entry was

not impaired in the SLC35B2^{KO} cells, we deduced that HS was involved in the viral RNA synthesis or protein translation. The DENV2 RNA and protein levels were also decreased in the HS-deficient cells, while we could not conclude that its replication was regulated by HS because the entry of DENV virions was largely inhibited. Although HS does not play a role in the ZIKV entry, it promotes the viral replication. The detailed underlying mechanism how HS promotes viral replication remains to be elucidated.

Consistent with previous notion that flaviviruses manipulate the cell death for their infection, we did not observe a rapid and strong cell death of A549 cells upon infection of ZIKV and DENV2 (Okamoto et al., 2017; Vicenzi et al., 2018). Nonetheless, the treatment of apoptosis or necrosis inhibitor, especially their combination, were able to increase the cell viabilities of the control cells, indicating that the apoptosis and necrosis did occur in A549 cells upon ZIKV or DENV2 infection, though at a low level. Interestingly, the ZIKV infection cause much less cytopathic effect in the HS deficient cells, implying that HS is involved in the cell death pathway. This finding was consistent with a recent work showing that heparin prevents virus-induced cell death of human neural progenitor cells (Ghezzi et al., 2017). Moreover, the necrosis inhibitor, but not the apoptosis inhibitor, enhanced the cell viabilities in the ZIKV-infected SLC35B2^{KO} cells, suggesting that the type of cell death regulated by HS was apoptosis, rather than necrosis. Regarding the mechanism that HS promotes the apoptosis induced by ZIKV and DENV2, we hypothesized that the viral replication products, including viral RNAs or proteins could be potent stimuli of apoptosis, such as the viral NS3 and NS2B3 that has been shown to induce apoptosis by DENV (Okamoto et al., 2017; Shafee and AbuBakar, 2003; Vicenzi et al., 2018). Therefore, the lower levels of viral RNAs and proteins produced in the SLC35B2^{KO} cells result in less cell death.

In addition, since HS and heparin bind to a number of pro-apoptotic cytokines and growth factors such as IFN-γ, TNF-α, and IL-8 (Lortat-Jacob, 2006; Salas et al., 2000), we have tested the levels of these cytokines in response to ZIKV infection by qRT-PCR and microarray analysis. No significant induction of IFN-γ, TNF-α, and IL-8 was detected, but the level of IFN-β was induced by 330-fold, which is consistent with Li's report (Li et al., 2017). However, the IFN-β treatment alone did not lead to the apoptosis of A549 cell within 24 h (Fig. 7). Overall, these observations exclude the possibility that HS mediates the apoptosis of infected A549 cells by binding to the proapoptotic cytokines.

The observations that the cytopathic effect was abolished in the ZIKV-infected SLC35B2^{KO} cells, and the inhibition of apoptosis and necrosis rescued the viral yields, promoted us to propose that HS was recruited by ZIKV for its RNA replication or protein synthesis, triggering a series of cell responses including programmed cell death; in turn, the cell death plays a protective role in inhibiting viral replication and transmission. This explanation helps to illustrate the phenomenon that in the SLC35B2^{KO} cells, the early viral RNA and protein levels of ZIKV and DENV2 were largely inhibited, while the amounts of viral progenies at 24 h p.i. were not correspondingly reduced.

In summary, our work demonstrated that the HS is not required for the viral attachment of ZIKV. But HS is involved in the ZIKV replication, and mediates the apoptosis induced by virus infection. These findings not only clarify the role of HS in the DENV and ZIKV entry, but also reveal new roles of HS in the interaction between virus and cells. Further investigations on the molecular mechanisms will advance our understanding of the ZIKV life cycle.

Acknowledgement

This work was supported by National Natural Science Foundation of China [grant number 81371794], Guangdong Science and Technology Department [grant number 2017A050501012, 2018A050506029], Natural Science Foundation of Guangdong Province [grant number 2017A030313504], and Fundamental Research Funds for the Central Universities [grant number 17ykjc01].

References

Balkwill, F., Taylor-Papadimitriou, J., 1978. Interferon affects both G1 and S + G2 in cells stimulated from quiescence to growth. Nature 274, 798–800.
Byrnes, A.P., Griffin, D.E., 1998. Binding of Sindbis virus to cell surface heparan sulfate. J. Virol. 72, 7349–7356.
Chawla-Sarkar, M., Lindner, D.J., Liu, Y.F., Williams, B.R., Sen, G.C., Silverman, R.H., Borden, E.C., 2003. Apoptosis and interferons: role of interferon-stimulated genes as mediators of apoptosis. Apoptosis 8, 237–249.
Chen, H.L., Her, S.Y., Huang, K.C., Cheng, H.T., Wu, C.W., Wu, S.C., Cheng, J.W., 2010. Identification of a heparin binding peptide from the Japanese encephalitis virus envelope protein. Biopolymers 94, 331–338.
Chen, Y., Maguire, T., Hileman, R.E., Fromm, J.R., Esko, J.D., Linhardt, R.J., Marks, R.M., 1997. Dengue virus infectivity depends on envelope protein binding to target cell heparan sulfate. Nat. Med. 3, 866–871.
Feldman, S.A., Audet, S., Beeler, J.A., 2000. The fusion glycoprotein of human respiratory syncytial virus facilitates virus attachment and infectivity via an interaction with cellular heparan sulfate. J. Virol. 74, 6442–6447.
Ferguson, M.C., Saul, S., Fragkoudis, R., Weisheit, S., Cox, J., Patabendige, A., Sherwood, K., Watson, M., Merits, A., Fazakerley, J.K., 2015. Ability of the encephalitic arbovirus semliki forest virus to cross the blood-brain barrier is determined by the charge of the E2 glycoprotein. J. Virol. 89, 7536–7549.
Fry, E.E., Lea, S.M., Jackson, T., Newman, J.W., Ellard, F.M., Blakemore, W.E., Abu-Ghazaleh, R., Samuel, A., King, A.M., Stuart, D.I., 1999. The structure and function of a foot-and-mouth disease virus-oligosaccharide receptor complex. EMBO J. 18, 543–554.
Germi, R., Crance, J.M., Garin, D., Guimet, J., Lortat-Jacob, H., Ruigrok, R.W., Zarski, J.P., Drouet, E., 2002. Heparan sulfate-mediated binding of infectious dengue virus type 2 and yellow fever virus. Virology 292, 162–168.
Ghezzi, S., Cooper, L., Rubio, A., Pagani, I., Capobianchi, M.R., Ippolito, G., Pelletier, J., Meneghetti, M.C.Z., Lima, M.A., Skidmore, M.A., Broccoli, V., Yates, E.A., Vicenzi, E., 2017. Heparin prevents Zika virus induced-cytopathic effects in human neural progenitor cells. Antivir. Res. 140, 13–17.
Goodfellow, I.G., Sioofy, A.B., Powell, R.M., Evans, D.J., 2001. Echoviruses bind heparan sulfate at the cell surface. J. Virol. 75, 4918–4921.
Hamel, R., Dejarnac, O., Wichit, S., Ekchariyawat, P., Neyret, A., Luplertlop, N., Perera-Lecoin, M., Surasombatpattana, P., Talignani, L., Thomas, F., Cao-Lormeau, V.M., Choumet, V., Briant, L., Despres, P., Amara, A., Yssel, H., Misse, D., 2015. Biology of Zika virus infection in human skin cells. J. Virol. 89, 8880–8896.
Kim, S.Y., Zhao, J., Liu, X., Fraser, K., Lin, L., Zhang, X., Zhang, F., Dordick, J.S., Linhardt, R.J., 2017. Interaction of Zika virus envelope protein with glycosaminoglycans. Biochemistry 56, 1151–1162.
Kreuger, J., Kjellen, L., 2012. Heparan sulfate biosynthesis: regulation and variability. J. Histochem. Cytochem. 60, 898–907.
Li, C., Deng, Y.Q., Wang, S., Ma, F., Aliyari, R., Huang, X.Y., Zhang, N.N., Watanabe, M., Dong, H.L., Liu, P., Li, X.F., Ye, Q., Tian, M., Hong, S., Fan, J., Zhao, H., Li, L., Vishlaghi, N., Buth, J.E., Au, C., Liu, Y., Lu, N., Du, P., Qin, F.X., Zhang, B., Gong, D., Dai, X., Sun, R., Novitch, B.G., Xu, Z., Qin, C.F., Cheng, G., 2017. 25-hydroxycholesterol protects host against Zika virus infection and its associated microcephaly in a mouse model. Immunity 46, 446–456.
Lin, C.L., Chung, C.S., Heine, H.G., Chang, W., 2000. Vaccinia virus envelope H3L protein binds to cell surface heparan sulfate and is important for intracellular mature virion morphogenesis and virus infection in vitro and in vivo. J. Virol. 74, 3353–3365.
Lortat-Jacob, H., 2006. Interferon and heparan sulphate. Biochem. Soc. Trans. 34, 461–464.
Maslow, J.N., 2017. Vaccines for emerging infectious diseases: lessons from MERS coronavirus and Zika virus. Hum. Vaccine Immunother. 13, 2918–2930.
Miner, J.J., Diamond, M.S., 2017. Zika virus pathogenesis and tissue tropism. Cell Host Microbe 21, 134–142.
Murakami, S., Takenaka-Uema, A., Kobayashi, T., Kato, K., Shimojima, M., Palmarini, M., Horimoto, T., 2017. Heparan sulfate proteoglycan is an important attachment factor for cell entry of akabane and schmallenberg viruses. J. Virol. 91.
Oh, Y., Zhang, F., Wang, Y., Lee, E.M., Choi, I.Y., Lim, H., Mirakhori, F., Li, R., Huang, L., Xu, T., Wu, H., Li, C., Qin, C.F., Wen, Z., Wu, Q.F., Tang, H., Xu, Z., Jin, P., Song, H., Ming, G.L., Lee, G., 2017. Zika virus directly infects peripheral neurons and induces cell death. Nat. Neurosci. 20, 1209–1212.
Okamoto, T., Suzuki, T., Kusakabe, S., Tokunaga, M., Hirano, J., Miyata, Y., Matsuura, Y., 2017. Regulation of apoptosis during flavivirus infection. Viruses 9.
Pierson, T.C., Diamond, M.S., 2018. The emergence of Zika virus and its new clinical syndromes. Nature 560, 573–581.
Ran, F.A., Hsu, P.D., Wright, J., Agarwala, V., Scott, D.A., Zhang, F., 2013. Genome engineering using the CRISPR-Cas9 system. Nat. Protoc. 8, 2281–2308.
Riblett, A.M., Blomen, V.A., Jae, L.T., Altamura, L.A., Doms, R.W., Brummelkamp, T.R., Wojcechowskyj, J.A., 2016. A haploid genetic screen identifies heparan sulfate proteoglycans supporting rift valley fever virus infection. J. Virol. 90, 1414–1423.
Richard, A.S., Shim, B.S., Kwon, Y.C., Zhang, R., Otsuka, Y., Schmitt, K., Berri, F., Diamond, M.S., Choe, H., 2017. AXL-dependent infection of human fetal endothelial cells distinguishes Zika virus from other pathogenic flaviviruses. Proc. Natl. Acad. Sci. USA 114, 2024–2029.
Roderiquez, G., Oravecz, T., Yanagishita, M., Bou-Habib, D.C., Mostowski, H., Norcross, M.A., 1995. Mediation of human immunodeficiency virus type 1 binding by interaction of cell surface heparan sulfate proteoglycans with the V3 region of envelope gp120-gp141. J. Virol. 69, 2233–2239.

Saiz, J.C., Oya, N.J., Blazquez, A.B., Escribano-Romero, E., Martin-Acebes, M.A., 2018. Host-directed antivirals: a Realistic alternative to fight Zika virus. Viruses 10.
Salas, A., Sans, M., Soriano, A., Reverter, J.C., Anderson, D.C., Pique, J.M., Panes, J., 2000. Heparin attenuates TNF-alpha induced inflammatory response through a CD11b dependent mechanism. Gut 47, 88–96.
Sasaki, M., Anindita, P.D., Ito, N., Sugiyama, M., Carr, M., Fukuhara, H., Ose, T., Maenaka, K., Takada, A., Hall, W.W., Orba, Y., Sawa, H., 2018. The role of heparan sulfate proteoglycans as an attachment factor for rabies virus entry and infection. J. Infect. Dis. 217, 1740–1749.
Shafee, N., AbuBakar, S., 2003. Dengue virus type 2 NS3 protease and NS2B-NS3 protease precursor induce apoptosis. J. Gen. Virol. 84, 2191–2195.
Shan, C., Xie, X., Shi, P.Y., 2018. Zika virus vaccine: progress and challenges. Cell Host Microbe 24, 12–17.
Silva, L.A., Khomandiak, S., Ashbrook, A.W., Weller, R., Heise, M.T., Morrison, T.E., Dermody, T.S., 2014. A single-amino-acid polymorphism in Chikungunya virus E2 glycoprotein influences glycosaminoglycan utilization. J. Virol. 88, 2385–2397.
Summerford, C., Samulski, R.J., 1998. Membrane-associated heparan sulfate proteoglycan is a receptor for adeno-associated virus type 2 virions. J. Virol. 72, 1438–1445.
Tan, C.W., Poh, C.L., Sam, I.C., Chan, Y.F., 2013. Enterovirus 71 uses cell surface heparan sulfate glycosaminoglycan as an attachment receptor. J. Virol. 87, 611–620.
Tan, C.W., Sam, I.C., Chong, W.L., Lee, V.S., Chan, Y.F., 2017. Polysulfonate suramin inhibits Zika virus infection. Antivir. Res. 143, 186–194.
Tanaka, A., Tumkosit, U., Nakamura, S., Motooka, D., Kishishita, N., Priengprom, T., Sa-Ngasang, A., Kinoshita, T., Takeda, N., Maeda, Y., 2017. Genome-wide screening uncovers the significance of n-sulfation of heparan sulfate as a host cell factor for chikungunya virus infection. J. Virol. 91.
Vicenzi, E., Pagani, I., Ghezzi, S., Taylor, S.L., Rudd, T.R., Lima, M.A., Skidmore, M.A., Yates, E.A., 2018. Subverting the mechanisms of cell death: flavivirus manipulation of host cell responses to infection. Biochem. Soc. Trans. 46, 609–617.
Yura, Y., Iga, H., Kondo, Y., Harada, K., Tsujimoto, H., Yanagawa, T., Yoshida, H., Sato, M., 1992. Heparan sulfate as a mediator of herpes simplex virus binding to basement membrane. J. Investig. Dermatol. 98, 494–498.
Zhang, X., Shi, J., Ye, X., Ku, Z., Zhang, C., Liu, Q., Huang, Z., 2017. Coxsackievirus A16 utilizes cell surface heparan sulfate glycosaminoglycans as its attachment receptor. Emerg. Microbes Infect. 6, e65.